Patterned microlens array for efficiency improvement of small-pixelated organic light-emitting devices

Hoang-Yan Lin[1], Yu-Hsuan Ho[1], Juin-Haw Lee[1], Kuan-Yu Chen[1], Jheng-Hao Fang[2], Sheng-Chih Hsu[1], Mao-Kuo Wei[2]*, Hung-Yi Lin[3], Jen-Hui Tsai[3] and Tung-Chuan Wu[3]

[1] *Graduate Institute of Photonics and Optoelectronics and Department of Electrical Engineering, National Taiwan University, Taipei, Taiwan 106, Republic of China*

[2] *Institute of Opto-Electronic Engineering and Department of Materials Science and Engineering, National Dong Hwa University, Hualien, Taiwan 974, Republic of China*

mkwei@mail.ndhu.edu.tw

[3] *Mechanical and Systems Research Laboratories, Industrial Technology Research Institute, Hsinchu, Taiwan 310, Republic of China*

Abstract: In this paper, we experimentally and theoretically investigated the optical characteristics of organic light-emitting devices (OLEDs), having different pixel sizes and attached with patterned microlens array films. For a regular microlens array, though it can extract the waveguiding light and increase luminous current efficiency for a large-pixelated OLED, we observed that it decreases the luminance to an even lower level than that of the planar OLED as its pixel size is close to the microlens dimension. Although a microlens can effectively outcouple the light rays originally at incident angles larger than the critical angle, it also can impede the outcoupling for the light rays originally at incident angles smaller than the critical angle. Enhancement or reduction of the light extraction depends on the relative positions of the light emitting point and the microlens. Therefore, we proposed a center-hollowed microlens array, of which the microlenses directly upon the pixel are removed, and proved that it can increase the luminous current efficiency and luminous power efficiency of a small-pixelated OLED. By attaching this patterned microlens array, 87% of luminance enhancement in the normal direction was observed for a 0.1×0.1 mm^2 OLED pixel. On the other hand, a regular microlens array resulted in 4% decrease under the same condition.

OCIS codes: (080.3630) Lenses; (230.3990) Microstructure devices.

Reference and links

1. M.-H. Lu and J. C. Sturm, “Optimization of external coupling and light emission in organic light-emitting devices: modeling and experiment,” J. Appl. Phys. **91**, 595-604 (2002).
2. S. Möller and S. R. Forrest, “Improved light out-coupling in organic light-emitting diodes employing ordered microlens arrays,”J. Appl. Phys. **91**, 3324-3327 (2002).
3. M.-K. Wei and I-L. Su, “Method to evaluate the enhancement of luminance efficiency in planar OLED light emitting devices for microlens array,” Opt. Express **12**, 5777-5782 (2004).
4. H. Peng, Y. L. Ho, X.-J. Yu, M. Wong, and H.-S. Kwok, “Coupling efficiency enhancement in organic light-emitting devices using microlens array-theory and experiment,” J. Display Technol. **1**, 278-282 (2005).
5. J. Lim, S. S. Oh, D. Y. Kim, S. J. Cho, I. T. Kim, S. H. Han, H. Takezoe, E. H. Choi, G.. S. Cho, S. O. Kang, and B. Park, “Enhanced out-coupling factor of microcavity organic light-emitting devices with irregular microlens array,” Opt. Express **14**, 6564-6571 (2006).
6. Y. Sun and S. R. Forrest, “Organic light emitting devices with enhanced outcoupling via microlenses fabricated by imprint lithography,” J. Appl. Phys. **100**, 073106 (2006).
7. M.-K. Wei, I-L. Su, Y.-J. Chen, M. Chang, H.-Y. Ling, and T.-C. Wu, “The influence of a microlens array on planar organic light-emitting devices,” J. Micromech. Microeng. **16**, 368-374 (2006).

8. H. Greiner, "Light extraction from organic light emitting diode substrates: simulation and experiment," Jpn. J. Appl. Phys. **46**, 4125-4137 (2007).
9. C.-J. Yang, S.-H. Liu, H.-H. Hsieh, C.-C. Liu, T.-Y. Cho, and C.-C. Wu, "Microcavity top-emitting organic light-emitting devices integrated with microlens arrays: simultaneous enhancement of quantum efficiency, cd/A efficiency, color performances, and image resolution," Appl. Phys. Lett. **91**, 253508 (2007).
10. T. Nakamura, N. Tsutsumi, N. Juni, and H. Fuji, "Thin-film waveguiding mode light extraction in organic electroluminescent device using high refractive index substrate," J. Appl. Phys. **97**, 054505 (2005).
11. M.-K. Wei, J.-H. Lee, H.-Y. Lin, Y.-H. Ho, K.-Y. Chen, C.-C. Lin, C.-F. Wu, H.-Y. Lin, J.-H. Tsai, and T.-C. Wu, "Efficiency improvement and spectral shift of an organic light-emitting device by attaching a hexagon-based microlens array," J. Opt. A: Pure Appl. Opt. **10**, 055302 (2008).
12. B. C. Krummacher, M. K. Mathai, V. Choong, S. A. Choulis, F. So, and A. Winnacker, "General method to evaluate substrate surface modification techniques for light extraction enhancement of organic light emitting diodes," J. Appl. Phys. **100**, 054702 (2006).
13. H.-Y. Lin, J.-H. Lee, M.-K. Wei, C.-L. Dai, C.-F. Wu, Y.-H. Ho, H.-Y. Lin, and T.-C. Wu, "Improvement of the outcoupling efficiency of an organic light-emitting device by attaching microstructured films," Opt. Commun. **275**, 464-9 (2007).
14. C.-H. Hsiao, C.-F. Lin, and J.-H. Lee, "Driving voltage reduction in white organic light-emitting devices from selectively doping in ambipolar blue emitting layer," J. Appl. Phys. **102**, 094508 (2007).
15. C. Y. Lin, S. C. Hsu, K. Y. Chen, H. Y. Lin, J. H. Lee, and M. K. Wei, "Low blur effect and high light extraction efficiency enhancement of organic light emitting displays with novel microstructure attachment," Soc. Inf. Display Tech. Digest **38**, 867-870 (2007).

1. Introduction

Due to the difference among the refractive indices of the substrate, anode, organic thin films, and the air, two waveguiding phenomena arise in the anode/organic layers and substrate of the organic light-emitting devices (OLEDs). Only 20-40% of the emitted light from the organic layers can escape into the air [1]. Among many methods, researchers used microlens arrays to increase both the luminous current efficiency and luminous power efficiency of the OLEDs, due to easiness and reliability in the fabrication process [2-11]. However, almost all the attention has been paid to the lighting applications in which the OLED's pixels are relatively larger than the microlenses.

Recently, the OLEDs have been successfully applied to the small- and medium-sized mobile electronic devices. The OLED displays comprise of hundreds of thousand to millions of pixels. Each pixel can be further divided into three sub-pixels, so its size is of the order of $100\times100\ \mu m^2$ which is close to that of microlenses. Thus, in this paper, we will study the influences of microlens arrays on the efficiency improvement and optical properties of the OLEDs with different pixel sizes.

Due to the corrugated structure of the microlenses, the incident angle from the substrate to the air is changed. The light rays at an incident angle larger than the critical angle in a planar OLED, as shown in the ray I of Fig. 1(a), can be coupled out by a microlens array attachment, as shown in the ray I of Fig. 1(b). This mechanism contributes to luminance ($lm/sr\cdot m^2$) enhancement. However, some of the light rays at an incident angle smaller than the critical angle in a planar case, as shown in the ray II of Fig. 1(a), can be reflected back to the glass substrate due to the microlens array attachment, as shown in the ray II of Fig. 1(b). In such case, the light extraction efficiency will be decreased by the microlenses and it is especially worse in the regions directly upon the pixels. Hence, the reported efficiency improvement [2-13] is in fact a balance between the enhancement and reduction of light extraction at different emission angles. For a large OLED pixel, microlenses extract the light from the area away from the measured region (as shown in the ray III of Fig. 1(c)), which contributes to a significant luminance enhancement. On the other hand, for a small OLED pixel ($< 0.5\times0.5$ mm^2), the emissive region is limited which means that only little waveguiding mode from the area away from the measured region can be extracted. However, microlenses can still diffract part of the light rays in the waveguiding mode for luminance enhancement, as described in the ray IV of Fig. 1(c). From our experiments, we observed a decrease in luminance, as compared to that of a planar OLED, due to the adverse effect of the microlenses to the light rays at small

#95390 - $15.00 USD Received 24 Apr 2008; revised 25 Jun 2008; accepted 6 Jul 2008; published 9 Jul 2008

emission angles. By removing the microlenses directly upon the pixel, an 87% increase was observed and it is much higher than the luminance enhancement of 33% by using a regular microlens array attachment on a large OLED pixel.

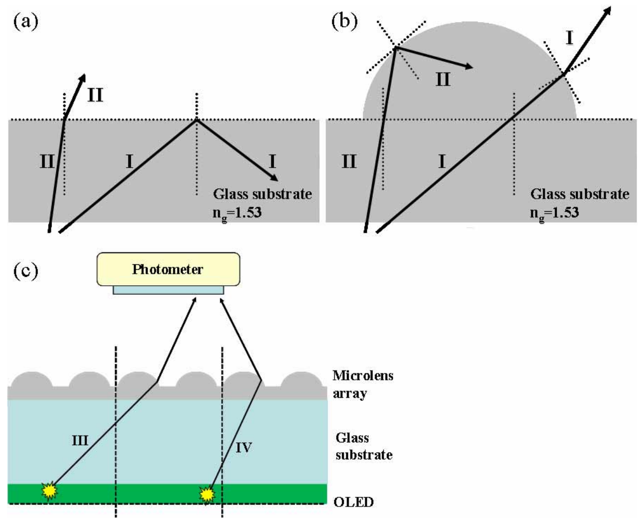

Fig. 1. The propagation of light rays in (a) the planar and (b) the corrugated substrates. (c) The schematics of the light rays in the waveguide mode extracted from an OLED with a microlens array attachment.

2. Experimental and simulation methods

The fabrication process of microlens arrays is illustrated in Fig. 2. A (100) silicon wafer was used as a substrate. The photoresist AZ P4620 was spun on the wafer. The photoresist disks were made through photolithographic process, followed by heating these disks at 230°C for 44 hrs to transform themselves into the shape of spherical caps. The liquid polydimethylsiloxane (PDMS) mixed with its hardener was poured onto the wafer and put in an oven to be thermally cured at 65°C for 4 hrs. The hardened PDMS mold with a concave microlens array on the mold surface was then released by peeling off the mold from the wafer. The liquid UV-curable PMMA was coated between the PDMS mold and PET film, followed by UV exposure at 1 J/cm^2 to harden the PMMA. Finally, a flexible PET film with the duplicated microlens array on the film surface was formed after separating the film from the mold.

The diameter and the sag of microlenses were set as 50 and 17 μm, respectively. The gap distance between two adjacent microlenses was set as 3 μm. The edge length of the base region and the gap distances of the photoresist plates (before thermal reflow) were measured by using a surface profiler (Tencor, Alpha-Step 500). The sag of microlenses was measured with a scanning electron microscope (Hitachi S3500). Two different patterned microlens arrays were used in this study. In the first pattern there are straightly arranged microlenses, which is called a regular microlens array. In the other it lacks 2×2 microlenses on the central region of an 80×80 regular microlens array, which is named a center-hollowed microlens array. The dimensions of the regular and center-hollowed microlens arrays are roughly 10×10 and 4.2×4.2 mm^2, respectively.

In this study, emitting layer of the OLED consists of a greenish-blue fluorescent emitter, 4,4’-bis[2-(4-(N,N-diphenylamino)phenyl)vinyl]biphenyl (DPAVBi) and complementary yellow fluorescent dopant, 5,6,11,12-tetraphenylnaphthacene (rubrene) doped in 9,10-bis(2’-naphthyl) anthracene (ADN) host for white light emission [14]. Organic materials for hole and electron transport layers are N,N’-diphenyl-N,N’-bis (1-naphthyl)-1,1’-biphenyl-4,4’-diamine

#95390 - $15.00 USD Received 24 Apr 2008; revised 25 Jun 2008; accepted 6 Jul 2008; published 9 Jul 2008

(NPB) and tris-(8-hydroxyquinoline) aluminum (Alq3), respectively. Device structure of the white OLED was ITO (130 nm)/NPB (40 nm)/ADN: 3% rubrene: 3% DPAVBi (10 nm)/ADN: 3% DPAVBi (35 nm)/Alq3 (15 nm)/LiF (1.2 nm)/Al (100 nm). The emissive area of the OLED varied from 0.1×0.1 to 10×10 mm^2 and the thickness of glass substrate was set at 0.7 mm. A source meter (Keithley 2400) was used to supply and monitor the driving current and voltage of the OLED. A spectroradiometer (Minolta CS-1000A) was used to measure the luminance, spectrum and CIE coordinates of the device in dark environment to minimize the influence of ambient light. For the angular-dependent luminance measurement, the device was fixed on a rotational stage, and the luminance was then measured at different viewing angles from 0° to 70°.

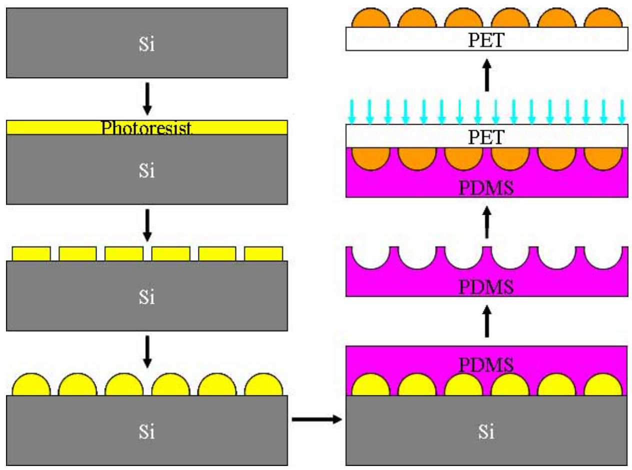

Fig. 2. The fabrication process of microlens arrays.

To investigate the influence of microlens arrays on the optical properties of the OLED, three differently arranged devices were used, as illustrated in Fig. 3. First, the OLED without any microlens arrays was driven at a voltage of 10 V and its luminance normal to the surface was measured as a reference. Regular and center-hollowed microlens arrays were in turn attached on the OLED by using refractive-index-matched oil (n ≈ 1.5). In this work, all the experiments were carried out by using the same driving current to the same OLED with and without microlens array attachments. In other words, the active areas, driving currents and voltages of the device were set the same in this study.

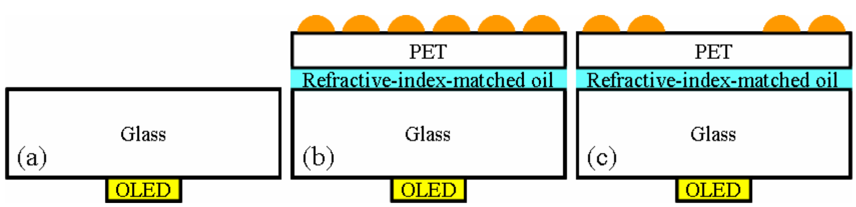

Fig. 3. The OLEDs attached (a) without, and with (b) a regular and (c) a center-hollowed microlens array.

To serve as a verification of the experimental results, the above three device models were built and a Monte Carlo ray tracing method was employed to simulate the propagation of light rays from a Lambertian OLED device by using commercial software LightTools™ from Optical Research Associates.

3. Results and discussion

When the OLEDs were covered with regular microlens arrays and driven at 10 V, the relative

#95390 - $15.00 USD Received 24 Apr 2008; revised 25 Jun 2008; accepted 6 Jul 2008; published 9 Jul 2008

luminance normal to the emitting surface was increased by raising the size of emitting regions, as depicted in Fig. 4(a). The relative luminance defined here was the ratio of the luminance of the OLED with a regular microlens array attachment to that of the OLED without any microlens array attachment. According to the reference [7, 11], this relative luminance is equal to the ratio of the luminous current efficiency of the OLED with a regular microlens array attachment to that of the OLED without any microlens array attachment. From the experiments, regular microlens arrays cannot enhance the luminous current efficiency as the size of emitting region of the OLED is smaller than 0.5×0.5 mm^2, but they do increase the luminous current efficiency when the size of the emitting region of the OLED becomes larger than 2×2 mm^2. In other words, for a small-pixelated OLED display, regular microlens array attachments may result in decrease of luminance at normal direction.

To confirm the experimental results obtained above, a ray-tracing method (LightTools software) was used to simulate the propagation of light rays from Lambertian OLEDs attached with regular microlens arrays. The reflectance of the cathode and the size of emitting regions of the OLED were set as 100% and from 0.1×0.1 to 5×5 mm^2, respectively. Figure 4(b) showed the relationship between the relative luminance normal to the emitting surface and the size of emitting regions of the OLED. The luminous current efficiency increased along with increasing the size of emitting region of the OLED. This trend was very similar to the experimental results except that the simulated values were greater than the experimental ones.

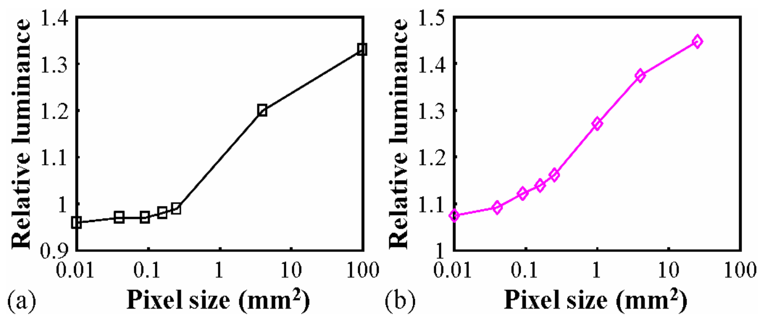

Fig. 4. The relationships between the relative luminance at normal direction and the pixel size of the OLEDs attached with regular microlens arrays: (a) experimental and (b) simulated results.

To increase the luminance for a small-pixelated OLED, a center-hollowed microlens array was proposed. Figure 5 showed a microphotograph of a center-hollowed microlens array on a transparent PET film. The diameter and the sag of microlenses were 50 and 17 μm, respectively, and the gap distance between two neighboring microlenses was 3 μm. Therefore, the area of the hollowed region on this array was 0.109×0.109 mm^2.

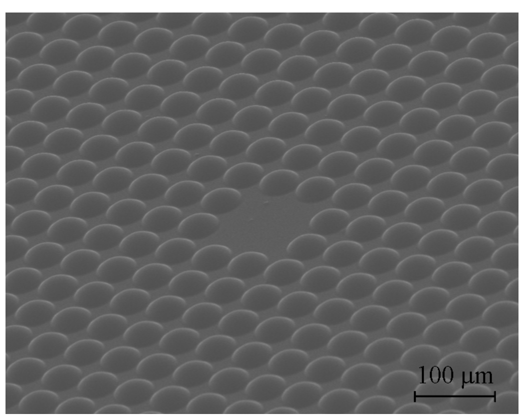

Fig. 5. Microphotograph of a duplicated center-hollowed microlens array (tilting angle: 60°).

#95390 - $15.00 USD Received 24 Apr 2008; revised 25 Jun 2008; accepted 6 Jul 2008; published 9 Jul 2008

For the sake to find the influence of this center-hollowed microlens array on the luminance enhancement of the device, five different emission areas of the OLEDs were used: 0.1×0.1, 0.2×0.2, 0.3×0.3, 0.4×0.4 and 0.5×0.5 mm^2. When the center-hollowed microlens array was attached in turn to the OLEDs, the luminance normal to the emitting surface increased with decreasing the emission area, as depicted in Fig. 6. The maximal gain of the luminance is reached when the emission area of the OLED, 0.1×0.1 mm^2, approximately equals the hollowed area on the patterned microlens array. Thus, the OLED having an emission area of 0.1×0.1 mm^2 was used in the following topics.

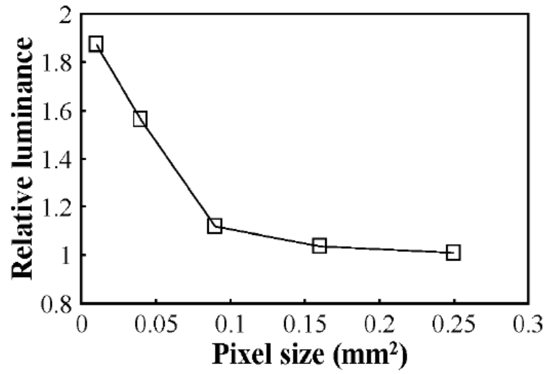

Fig. 6. The behavior of the relative luminance at normal direction versus the pixel size of the OLEDs attached with the same patterned microlens array.

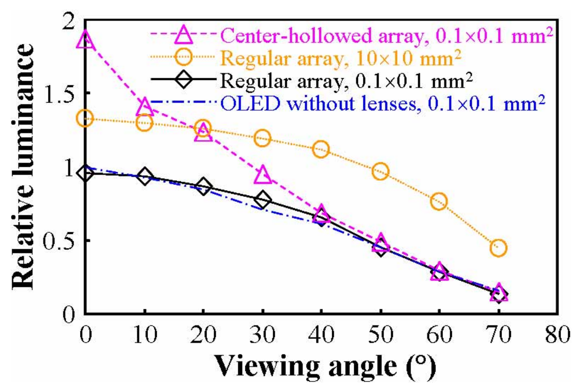

Fig. 7. The angular-dependent luminance of the OLED attached with a regular microlens array or with a center-hollowed array.

Figure 7 showed the relative luminance at different viewing angles of the OLED having a small emission area of 0.1×0.1 mm^2 without and attached by regular and center-hollowed microlens arrays. Besides, the relative luminance of a large OLED pixel, i.e. 10×10 mm^2, attached by a regular microlens array was also shown for comparison. Denominator of the relative luminance here is the luminance at the normal direction of the OLED without any microlens array attachment. Experimental results showed that both the angular-dependent luminance of the small OLED pixel without and with a regular microlens array was similar. It also appeared that regular microlens arrays do not help small OLED pixels, as shown in Fig. 4(a), in fact, are detrimental. On the other hand, when attaching a center-hollowed microlens array, 87% enhancement in luminance can be obtained. By integrating over the whole viewing angles, the luminous power efficiency of the OLED with the regular and center-hollowed microlens arrays were increased by 3% and 22%, respectively. When attaching a regular microlens array film on a large OLED pixel, one can see the luminance enhancement especially at large viewing angles and it comes from the extraction of the waveguiding mode

[11]. One can note that the luminance enhancement at normal direction is 33% for a large OLED pixel with a regular microlens array, which is less than the value of the OLED with a center-hollowed microlens array, due to the removal of those microlenses impeding light extraction. When integrating over the whole viewing angles, improvement of the luminous power efficiency for the large OLED pixel is 42%. Such a high value comes from the contribution of light extraction at large viewing angles.

The reason that a center-hollowed microlens array can enhance more efficiency of the OLED than a regular microlens array may be explained by the emitting images of the OLEDs illustrated in Fig. 8. When the OLED without microlenses array attachment was driven, a square enlarged image of the pixel was shown in Fig. 8(a). It is formed by the light rays at incident angles smaller than the critical angle (~41.8°). The other light rays at incident angles greater than the critical angle will be totally reflected back and waveguided in the glass substrate. When the OLED was attached by a center-hollowed microlens array, its emitting image, as depicted in Fig. 8(b), was slightly different from that in Fig. 8(a). Most of the central part is contributed from the light rays at incident angles smaller than the critical angle, which was the same as that of the OLED without microlens array attachment. In the region surrounding the pixel, however, some of the light rays originally at incident angles larger than the critical angle were coupled out into the air by the microlenses. Therefore, a center-hollowed microlens can strongly increase the efficiency of the OLED. When the OLED was attached by a regular microlens array, its emitting image, as described in Fig. 8(c), was quite different from Figs. 8(a) and (b). Based on the same mechanism, the amount of the light rays coupled out in the region surrounding the pixel was very similar to that of the OLED attached by a center-hollowed microlens array. However, in the central part, the propagation of the light rays of the OLED attached by a regular microlens array was very different from that of the OLED without microlens array attachment or attached with a center-hollowed microlens array. The light rays could only pass through the gap region among microlenses and the middle regions of microlenses into the air, but were reflected back at near the rims of microlenses. The efficiency improvement of the OLED by a regular microlens array is thus less than that by a center-hollowed microlens array.

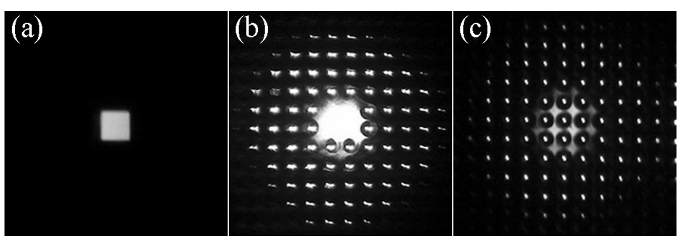

Fig. 8. Photographs of the OLED attached (a) without microlenses and with (b) a center-hollowed or (c) a regular microlens array.

Figure 9 showed the spectra and CIE coordinates of the OLED without and attached with microlens arrays. The OLED without any microlenses had three peak emitting wavelengths at 468, 497 and 585 nm, and its CIE coordinate was (0.3302, 0.3349) when driven at 10 V. The peak emitting wavelengths were not changed when the OLED was attached with a regular or a center-hollowed microlens array, but the relative intensity of the shorter wavelengths of the OLED attached with a regular microlens array was less than that of the OLED attached with a center-hollowed microlens array, as shown in Fig. 9(a). It means that the OLED had more red shift when attached with a regular microlens array than attached with a center-hollowed microlens array, which is confirmed by their CIE indices, as depicted in Fig. 9(b). This can be explained by the fact that the microlenses surrounding the OLED pixel help to extract the red light components originally trapped due to the material dispersion and the microlenses directly upon the OLED pixel prevent to extract the blue light components due to the thin film

#95390 - $15.00 USD Received 24 Apr 2008; revised 25 Jun 2008; accepted 6 Jul 2008; published 9 Jul 2008

structure [11, 12].

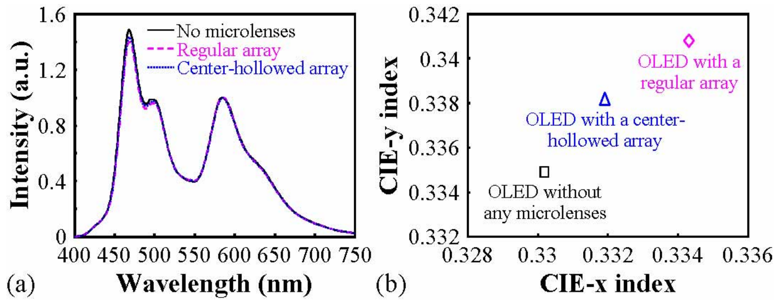

Fig. 9. (a) The spectra and (b) CIE indices of the OLED attached without and with microlens arrays.

To utilize a microlens array on an OLED inevitably results in pixel blurring, as shown in Figs. 8(b) and (c), this is because the light rays are outcoupled from the non-emissive region. Hence, microlenses are more suitable for OLED lighting than display applications. Due to low conductivity of ITO, assisted anode (such as Al and Ag) is typically used to reduce the ohmic loss especially for large-sized lighting devices. These electrode materials are opaque which limits the aperture ratio of the devices. By appropriate layout of the OLED and microlenses for lighting application, it may be possible to reduce the driving voltage and to increase the outcoupling at the same time. For the OLED display, unfortunately, image quality inevitably degrades with the attachment of microlenses. Comparing Figs. 8(b) and (c), light intensity outside the pixel region is the same. However, intensity inside the pixel is stronger in the center-hollowed case, as mentioned before, which results in a smaller pixel blur width as compared to that resulted from the regular microlens array [15]. One may expect the pixel blurring is alleviated by removing the microlens upon the emissive region. In Figs. 8(b) and (c), the pixel blurring is about 600 μm in diameter, which is even larger than pixel dimensions of a small- or medium-sized display (2” to 20”). For a TV, the pixel size is as large as 1 mm that means this blurring may be acceptable.

4. Conclusions

It was found that a regular microlens array cannot efficiently improve the efficiency of the OLED with a small emitting region. The greater the emitting region of the OLED is, the more the efficiency improvement of the OLED a regular microlens array can gain. To increase the efficiency of the OLED having a small pixel size, we proposed a center-hollowed microlens array. This microlens array can not only strongly enhance the luminous current efficiency but also improve the luminous power efficiency of the OLED. In addition, the red shift of the spectrum of the OLED is also smaller when attached with a center-hollowed microlens array than with a regular microlens array.

Acknowledgments

The authors gratefully acknowledge the financial support given by the National Science Council of the Republic of China under projects NSC 96-2221-E-002-118, NSC 96-2221-E-002-126, and NSC 96-2221-E-259-030. We also acknowledge the financial support by Chung-Shan Institute of Science and Technology of the Republic of China.